Since January 2020 Elsevier has created a COVID-19 resource centre with free information in English and Mandarin on the novel coronavirus COVID-19. The COVID-19 resource centre is hosted on Elsevier Connect, the company's public news and information website.

Informatics in Medicine Unlocked 27 (2021) 100807

Contents lists available at ScienceDirect

Informatics in Medicine Unlocked

journal homepage: www.elsevier.com/locate/imu

Impact of environmental transmission and contact rates on Covid-19 dynamics: A simulation study

H. Rwezaura [a], S.Y. Tchoumi [b,*], J.M. Tchuenche [c]

[a] Mathematics Department, University of Dar es Salaam, P.O. Box 35062, Dar es Salaam, Tanzania
[b] Department of Mathematics and Computer Sciences ENSAI, University of Ngaoundere, P.O. Box 455, Ngaoundere, Cameroon
[c] School of Computational and Communication Sciences and Engineering, Nelson Mandela African Institute of Science and Technology, P.O. Box 447, Arusha, Tanzania

ARTICLE INFO

Keywords:
Covid-19
Effective contact rate
Basic reproduction number
Indirect transmission

ABSTRACT

The emergence of the COVID-19 pandemic has been a major social and economic challenge globally. Infections from infected surfaces have been identified as drivers of Covid-19 transmission, but many epidemiological models do not include an environmental component to account for indirect transmission. We formulate a deterministic Covid-19 model with both direct and indirect transmissions. The computed basic reproduction number R_0 represents the average number of secondary direct human-to-human infections, and the average number of secondary indirect infections from the environment. Using Partial Rank Correlation Coefficient, we compute sensitivity indices of the basic reproductive number R_0. As expected, the most significant parameter to reduce initial disease transmission is the natural death rate of pathogens in the environment. Variation of the basic reproduction number for different values of direct and indirect transmissions are numerically investigated. Decreasing the effective direct human-to-human contact rate and indirect transmission from human-to-environment will decrease the spread of the disease as R_0 decreases and vice versa. Since the effective contact rate often accounted for as a factor of the force of infection and other interventions measures such as treatment rate are prominent features of infectious diseases, we consider several functional forms of the incidence function, and numerically investigate their potential impact on the long-term dynamics of the disease. Simulations results revealed some differences for the time and infection to reach its peak. Thus, the choice of the functional form of the force of infection should mainly be influenced by the specifics of the prevention measures being implemented.

1. Introduction

The 2019 coronavirus disease (Covid-19) caused by the severe acute respiratory syndrome coronavirus 2 (SARS-CoV-2) is a global public health concern worldwide [1], with serious health, social, and economic consequences, a crisis of unprecedented proportions [2]. The disease spreads through direct transmission (person-to-person), which has been the focus of most modeling studies [3]. While human-to-human transmission dynamics is well established, little attention has been provided to indirect transmission of the virus through surfaces such as door handles, at least from the mathematical standpoint. It is well documented that the SARS-CoV-2 can persist on hard surfaces and in the environment [3], and as such, environmental factors may have a great impact on the transmission dynamics of the disease [4]. We assume that infectious individuals are responsible for shedding the virus in the environment, and susceptible individuals could be infected by accidental contacts with the virus on surfaces [5].

Several studies have included the environment in their mathematical model, but they only considered the contribution of infectives shedding the virus in the environment, that is the role human play by releasing the virus into the environment by including an additional compartment for contaminated environment [6–11]. Specifically accounting for indirect human-to-environment transmission is important to investigate the impact this additional transmission route has on the long term dynamics of the disease. To address this gap, we include an additional force of infection to account for this indirect transmission [12,13]. With increase in the number of cases despite the strict non-pharmaceutical (prevention) interventions (wearing face mask, practicing social/physical distancing, and environmental disinfection) suggests the importance of investigating the impact of indirect transmission of Covid-19 by coupling the transmission dynamic of the virus in the environment to the direct transmission modeling pathway.

* Corresponding author.
E-mail address: sytchoumi83@gmail.com (S.Y. Tchoumi).

https://doi.org/10.1016/j.imu.2021.100807
Received 20 October 2021; Received in revised form 23 November 2021; Accepted 23 November 2021
Available online 6 December 2021

The proposed model is an improvement on the work in [12–14]. Given the current state of the pandemic, we include a vaccination class, with a vaccine waning rate. Motivated by the aforementioned, we develop a susceptible–vaccinated–exposed–infectious–recovered ($SVEIRS-P$) deterministic mathematical model for the transmission dynamic of Covid-19 incorporating both direct (human-to-human) transmission, indirect (human–environment–human) transmission from the environment. Because the virus can survive several days on different surfaces, investigating the potential impact played by indirect Covid-19 transmission through contaminated environment could be crucial to mitigate factors that intensify the spread of the virus.

Infections from infected surfaces have been identified as drivers of Covid-19 transmission, and a lot of money have been spent on disinfecting surfaces and work places. Yet, many epidemiological models do not include an environmental component to account for indirect transmission. To study the potential impact of this indirect transmission on the Covid-19 transmission dynamics, we formulate and analyze a mathematical model that incorporates the environmental component. Preventive non-pharmaceutical control interventions have been accounted for in the disease force of infection, specifically by including these as part of the effective contact rate. Disease transmission/contact parameter is generally incorporated into the force of infection. To this effect, we numerically investigate different functional forms of the contact and treatment rates when the basic reproduction number is either less or greater than unity, and highlight what their effect could be on the long-term dynamics the disease. The aim is to answer the following question: Can the choice of the functional forms of the contact and treatment rates influence the long term dynamics of the disease? To address this question, we performed numerous numerical simulations varying key parameters.

The rest of the paper is organized as follows. The proposed model is formulated and the basic reproduction number computed in Section 2. Variations of the basic reproduction number and the infected class for different values of these parameters are shown graphically in Section 3, along with the long term dynamics of various effective contact rates on the infection dynamics. The conclusion is provided in Section 4.

2. The model

We developed a simplistic caricature $SVEIRS-P$-type compartmental model that combines direct and indirect Covid-19 transmission, including vaccination and the dynamics of contaminated surfaces (environment). Direct or indirect transmission requires contact between an animal source and humans or contact with the pathogen in the environment.

Consider a homogeneously mixing within the population, i.e., individuals in the population have equal probability of contact with each other. Using a deterministic compartmental modeling approach to describe the disease transmission dynamics, the total population $N(t)$ at any time t is subdivided into several epidemiological classes depending on individuals health status: susceptible $S(t)$, vaccinated $V(t)$, exposed $E(t)$, infectious $I(t)$, and recovered $R(t)$. The pathogen in the environment is denoted as $P(t)$ (see Fig. 1).

$$\begin{cases} \frac{dS}{dt} = p\Pi + wV + \gamma R - \left(\lambda_S + \upsilon + \mu\right) S, \\ \frac{dV}{dt} = q\Pi + \upsilon S - \left(\lambda_V + w + \mu\right) V, \\ \frac{dE}{dt} = \lambda_S S + \lambda_V V - (\phi + \mu)E, \\ \frac{dI}{dt} = \phi E - (\tau + \mu + \delta)I, \\ \frac{dR}{dt} = \tau I - (\gamma + \mu)R, \\ \frac{dP}{dt} = \eta I - \mu_P P. \end{cases} \tag{1}$$

with initial conditions

$$S(0) \geq 0,\ V(0) \geq 0,\ E(0) \geq 0,\ I(0) \geq 0,\ R(0) \geq 0, P(0) \geq 0, \tag{2}$$

where

$\lambda_S = \frac{\beta_I I}{1+\alpha_1 I} + \frac{\beta_P P}{1+\alpha_2 P}$, and $\lambda_V = \frac{\sigma\beta_I I}{1+\alpha_1 I}$, and $p + q = 1$.

We choose a Holling type-II functional response based on the fact that, even though the spread of Covid-19 is rapid, there is (will) always (be) a saturation point. The type-II functional response captures this saturation/inhibitory effect as the number of infectives becomes large [15]. The constant parameters α_1, α_2 measure this saturation effect. In the expression $1 + \alpha_1 I$, we note that 1 represents the half saturation constant (often denoted by H), that is the concentration of Corona virus on surfaces that yields a 50% chance of contracting Covid-19 [15]. All model parameters, their description, values and sources are provided in Table 1.

There are multiple epidemiological indicators used for discussing the spread of diseases such as the basic reproductive number, a threshold parameter which indicates whether the disease is going to spread or die out.

2.1. Disease-free equilibrium and basic reproduction number

The disease-free equilibrium of the system (1) is given by $E^0 = \left(S^0, V^0, 0, 0, 0, 0\right)$ where

$$S^0 = \frac{\Pi[\mu p + w(p+q)]}{\mu(\mu+\upsilon+w)}, \quad \text{and} \quad V^0 = \frac{\Pi[\mu q + \upsilon(p+q)]}{\mu(\mu+\upsilon+w)}.$$

Using the next generation matrix method in [16], the associated next generation matrix and the rate of transfer of individuals of model system (1) are given by

$$\mathcal{F} = \begin{bmatrix} \frac{\beta_I IS}{1+\alpha_1 IS} + \frac{\beta_P PS}{1+\alpha_2 P} + \frac{\sigma\beta_I IV}{1+\alpha_1 I} \\ 0 \\ \eta I \end{bmatrix} \quad \text{and}$$

$$\mathcal{V} = \begin{bmatrix} -(\mu+\phi)E \\ \phi E - (\mu+\tau+\delta)I \\ -\mu_P P \end{bmatrix}.$$

Hence, the new infection terms F and the remaining transfer terms V are respectively given by

$$F = \begin{bmatrix} 0 & \beta_I(S^0+V^0) & \beta_P S^0 \\ 0 & 0 & 0 \\ 0 & \eta & 0 \end{bmatrix} \quad \text{and}$$

$$V = \begin{bmatrix} -(\mu+\phi) & 0 & 0 \\ \phi & -(\mu+\tau+\delta) & 0 \\ 0 & 0 & -\mu_P \end{bmatrix}.$$

Thus,

$$FV^{-1} = \begin{bmatrix} \frac{(S^0+V^0)\beta_1\phi}{(\delta+\mu+\tau)(\mu+\phi)} & \frac{(S^0+V^0)\beta_1}{\delta+\mu+\tau} & \frac{S\beta_2}{\mu_P} \\ 0 & 0 & 0 \\ \frac{\eta\phi}{(\delta+\mu+\tau)(\mu+\phi)} & \frac{\eta}{\delta+\mu+\tau} & 0 \end{bmatrix}.$$

The dominant eigenvalue or spectral radius of the next generation matrix FV^{-1} which represents the basic reproductive number is given

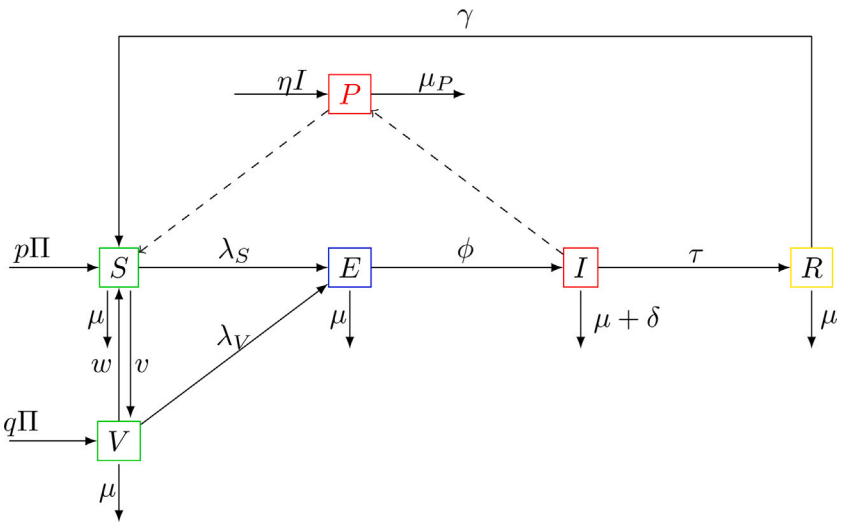

Fig. 1. Compartment diagram of the human component of the model.

by

$$R_0 = \frac{1}{2}\left[R_0^h + \sqrt{\left(R_0^h\right)^2 + 4R_0^P}\right], \tag{3}$$

where

$$R_0^h = \frac{\beta_I \phi(S^0 + V^0)}{(\delta+\mu+\tau)(\mu+\phi)}, \tag{4}$$

and

$$R_0^P = \frac{\beta_P \phi \eta S^0}{\mu_P(\delta+\mu+\tau)(\mu+\phi)}. \tag{5}$$

The expression of R_0 in (3) is made of two parts: the average number of secondary direct human-to-human infections, and the average number of secondary indirect infections from the environment.

The basic reproductive number denoted by R_0 which measures initial disease transmission is (a threshold value that characterizes the local asymptotic stability of the underlying dynamical system), and one of the most crucial quantities in infectious diseases [17]. It is defined as the average number of secondary infections generated by a single infectious individual over the duration of his infection, in an otherwise entirely susceptible/naive population [16]. The potential of an epidemic to spread very quickly or not is based on the classical behavior of R_0 being greater or less than unity [18]. Eq. (4) represents the infection from direct human-to-human contacts while Eq. (5) represents the infection contributed by indirect transmission through the environment. Similar expressions and interpretation of the basic reproduction number in Eq. (3) can be found in [19,20].

2.2. Sensitivity analysis of R_0

By construction, mathematical models (symbolic representations of real-life situation) inherit the loss of information. We perform sensitivity analysis by employing the Partial rank correlation coefficients (PRCCs) and the Latin hypercube scheme to identify model parameters that significantly impact disease transmission using the reproduction number R_0 as the response function. The sign of the PRCC indicates the specific qualitative relationship between the input parameter and R_0. Parameters with large PRCC are strongly correlated with the basic reproduction number R_0, that is, the larger the value of the PRCC, the larger is the contribution of the input parameter in the size of R_0.

Parameter sensitivity analysis suggests that the most impactful parameters include the inflow of individuals into the community (the per capita recruitment rate) Π, the effective disease transmission/contact rates β_I, β_P, the progression rate from exposed to infectious ϕ among others. As expected, that increasing the vaccination rate υ will decrease R_0, while increasing the vaccine waning rate will increase the value of R_0. Thus, early ranking the intervention measures based on their impact could ideally partially inform the process of prioritizing public health intervention measures to be implemented during the COVID-19. The PRCC analysis plot is depicted in Fig. 2.

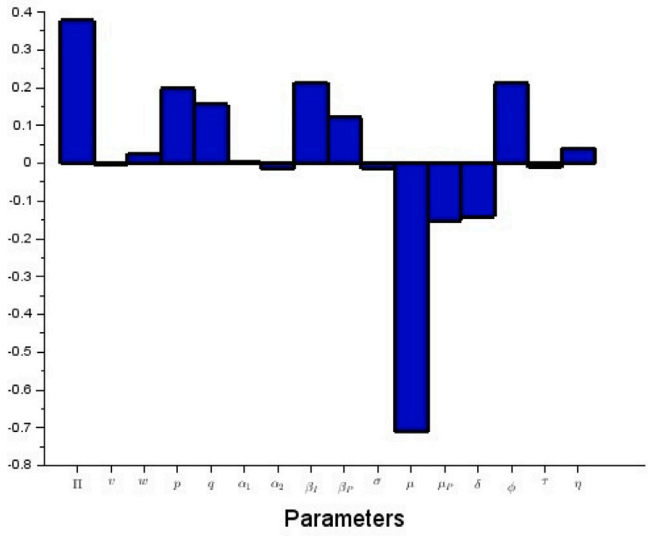

Fig. 2. Partial rank correlation coefficients for $n = 10{,}000$ simulations using the Latin hypercube sampling showing the impact of model parameters on the reproduction number R_0.

3. Numerical simulations

Graphical representations depicting the dynamical behavior of the model system (1) when the fundamental threshold parameter R_0 is either greater or less than unity are presented. All model parameter values used in our simulations are shown in Table 1.

3.1. Heat map of R_0 for different values of the parameters considered

The variation of the basic reproduction number R_0 for different daily values of direct and indirect contact rates β_I and β_P is shown in the heat map in Fig. 3. Decreasing the effective direct human-to-human

Table 1
Fundamental model parameter.

Parameter	Description	Value	Range	Reference
Π	Recruitment or inflow into the population	$\frac{1000}{59\times365}$		[21,22]
υ	Vaccination rate	0.45	$[10^{-5},\ 8\times10^{-2}]$	[23,24]
w	Vaccine waning rate	0.0001		Assumed
p	Fraction of recruited who are susceptible	0.9		
q	Fraction of recruited who are already vaccinated	0.1	[0, 0.99]	[23,24]
α_1	Proportion of interaction with an infectious individual	0.1		[12]
α_2	Proportion of interaction with an infectious environment	0.1		[12]
β_I	Rate of transmission from S to E due to contact with I	0.0115		[12]
β_P	Rate of transmission from S to E due to contact with P	0.00414		[12]
σ	Reduction of infectiousness of vaccinated	0.001		Assumed
μ	Natural death rate	$\frac{1}{59\times365}$		[12,21]
μ_P	Natural death rate of pathogens in the environment	0.1724		[12]
δ	Disease-induced death rate	0.0018		[12]
ϕ	Progression rate from E to I	0.09		[12]
τ	Recovery rate of infected individuals	0.05	$[\frac{1}{30},\ \frac{1}{4}]$	[12,25,26]
η	Rate of virus spread to environment by infectious individuals	0.1	$[\frac{1}{20},\ \frac{1}{10}]$	[12]

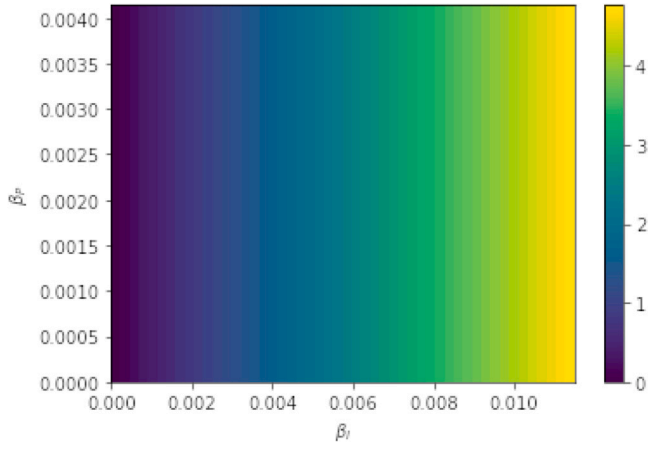

Fig. 3. Heat map of R_0 for different values of β_I and β_P.

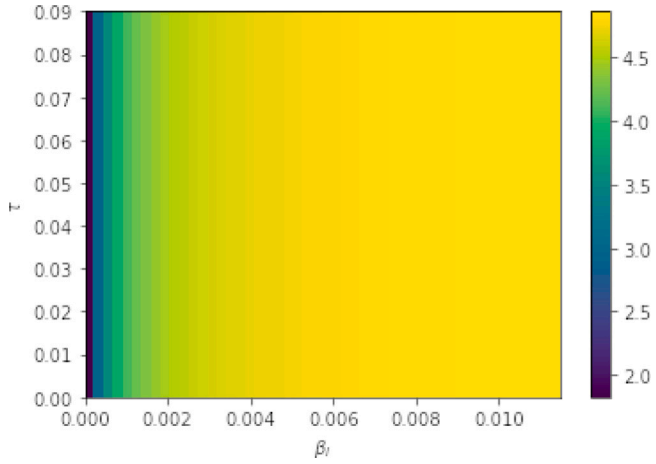

Fig. 4. Heat map of R_0 for different values of β_I and τ.

contact rate and indirect transmission from human-to-environment will decrease the spread of the disease as R_0 decreases and vice versa [27]. Similarly, the surface plot depicting the variation of R_0 for different values of direct transmission via the human-to-human contact rate β_I and treatment rate τ is shown in Fig. 4. Over broad regions of parameter space, as the contact rate increases, R_0 also increases, and consequently, the treatment level to mitigate the spread of the epidemic via reduction of the number of secondary infections caused by an infective during his entire period of infection increases.

Fig. 5 is the health map of the variations of the daily contact and vaccination rates β_I and υ. The more the contacts, the more the level of vaccination efforts necessary to control the epidemic. Fig. 6 depicts the impact of the vaccination waning immunity of the dynamics of the disease.

3.2. Long term dynamics of the infected component $I(t)$ with $R_0 > 1$ and $R_0 < 1$

Case 1: *Impact of indirect transmission* - The impact of indirect (environmental) transmission on the Covid-19 infection dynamics is graphically represented for $I(t)$ with and without direct environmental transmission (i.e., the environmental-induced force of infection $\frac{\beta_P P}{1+\alpha_2 P}$ is zero or not) when the basic reproduction number R_0 is either greater or less than unity. As expected, from Fig. 8, the introduction of environmental perturbations (transmission) has a clear impact on the disease dynamics as this increases the number of infected individuals [28]. Therefore, additional mitigation strategies should be put in place such as regularly disinfecting surfaces and hand sanitization (see Fig. 7).

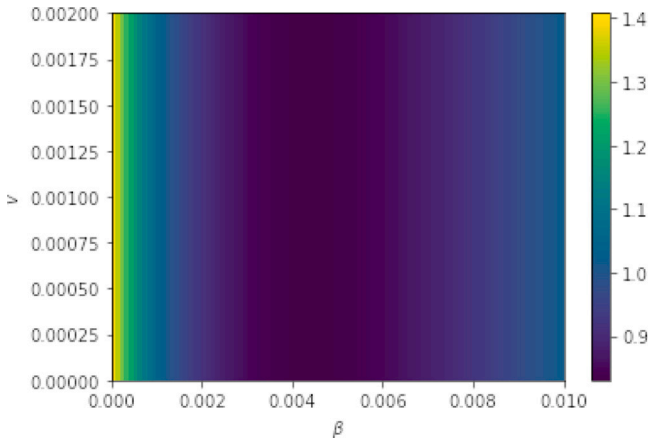

Fig. 5. Heat map of R_0 varying the value of direct contact and vaccination rates β_I and υ.

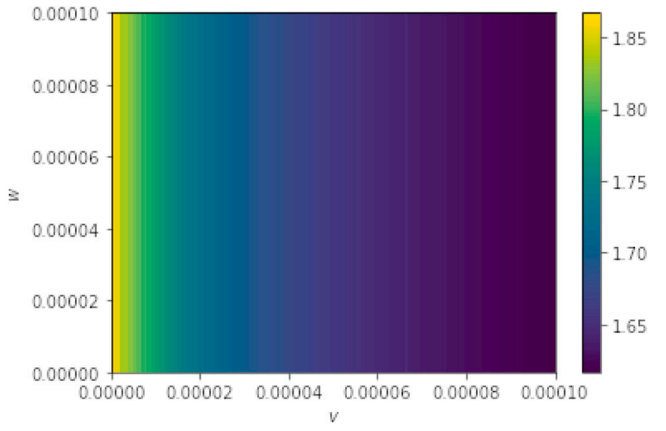

Fig. 6. Heat map of R_0 for different values of vaccination and waining immunity rates υ and w.

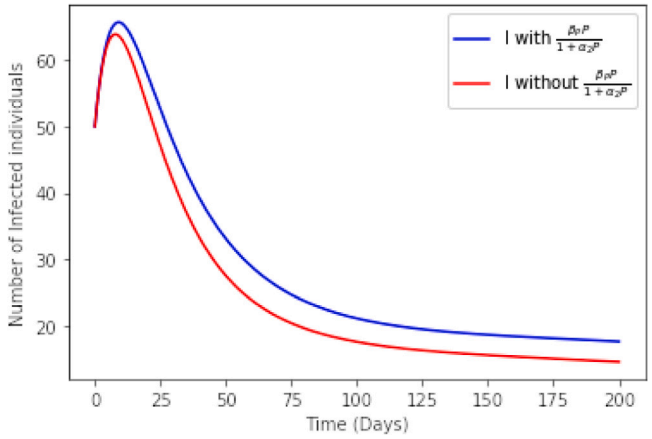

Fig. 7. Dynamics of infected individuals I with and without indirect transmission when $R_0 = 0.49$.

An epidemic is a function of environmental factors and a contact structure that varies over time, which in turn leads to varying transmission potential of an infection. Different forms of the transmission rates β, from constant to dynamic contact rate abound in the literature. We numerically investigate the impact of (some of) these contact rates on the long term dynamics of the disease. These are graphically represented below for the infective class only.

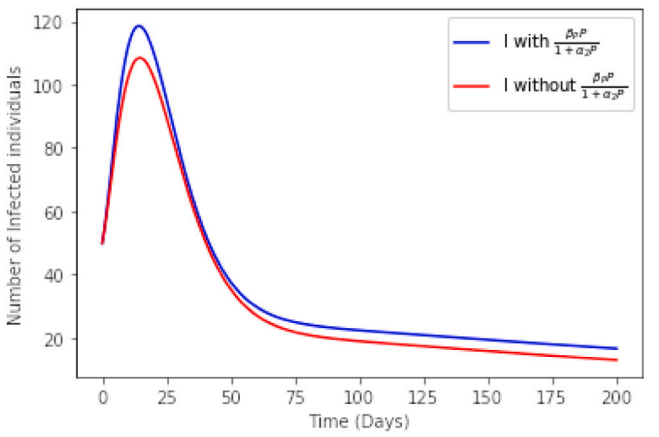

Fig. 8. Dynamics of infected individuals I with and without indirect transmission when $R_0 = 4.86$.

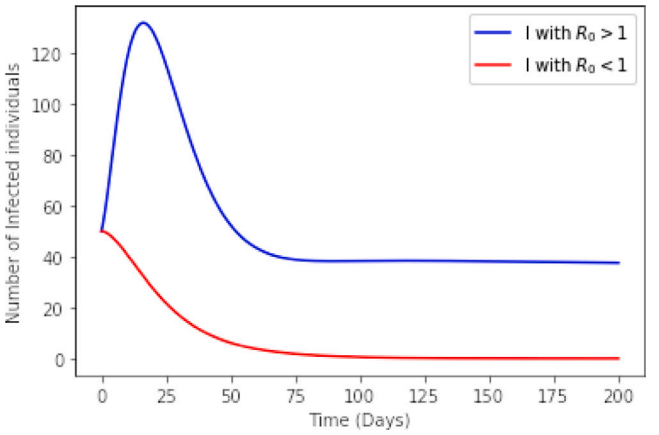

Fig. 9. Dynamics of infected individuals I with $\beta = \beta_0(1 - \alpha\xi)$ when $R_0 = 4.61$ and $R_0 = 0.48$.

Case 2: *Face masks vs. isolation of infectives and lock down* - While face masks have been highly successful in mitigating the spread of Covid-19, it has been noticed that fatigue is creeping in. We compare the impact of face masks and a combination of isolation of infectives and complete lock down. The latter prevention measure has very high economic consequences on people's daily life. Efficacy of mask usage at reducing the risk of direct transmission of Covid-19 has been included in the contact rate [29,30]. In this case the effective contact rate $\beta = \beta_0(1 - \alpha\xi)$, with $0 \leq \alpha, \xi \leq 1$, where $\xi = 0.5$ is the efficacy of face masks, $\alpha = 0.1$ is the proportion of those using face masks. If lock down and isolation of infectives are implemented in the community, these are accounted for in the model as part of the effective contact rate $\beta = \beta_0(1 - \zeta)(1 - \kappa)$, with $0 \leq \zeta, \kappa \leq 1$ [31]. The parameter $\zeta = 0.05$ represents the lock down rate of susceptible, while $\kappa = 0.05$ is the isolation rate of infectives. Although Figs. 9 and 10 are similar, the value of the reproduction number are slightly different as indicated in the figures' captions. This indicates that adhering and consistently wearing face masks somehow have a similar effect as when isolation of infectives and the stringent lock down measure are implemented.

The figures below are generated with $R_0 = 4.38$ and $R_0 = 0.45$.

Case 3: *Social/physical distancing, hand washing and face mask vs. time dependent contact rate* - Riyapan et al. [29] introduce the effect of physical distancing, hand washing and face masks wearing $\beta = \beta_0(1 - \zeta\xi)(1 - \kappa)(1 - \upsilon)$, with $0 \leq \zeta, \kappa, \upsilon \leq 1$, where $\zeta = 0.1$ is the proportion wearing face mask, $\xi 0.5$ is the efficacy of the face mask, $\kappa = 0.7$ the proportion practicing physical distancing, $\upsilon = 0.5$ is the

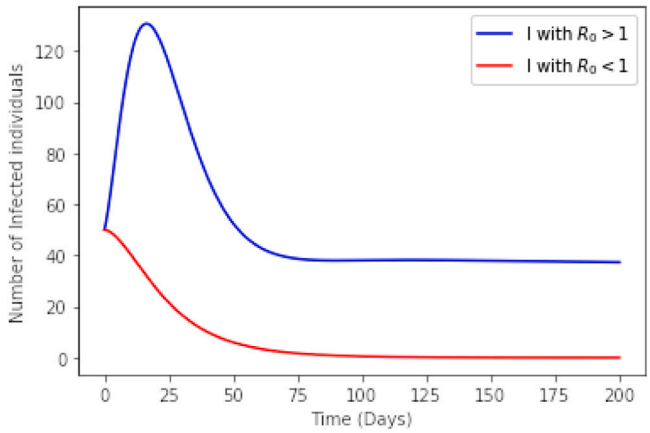

Fig. 10. Dynamics of infected individuals I with $\beta = \beta_0(1-\zeta)(1-\kappa)$ when $R_0 = 4.38$ and $R_0 = 0.45$.

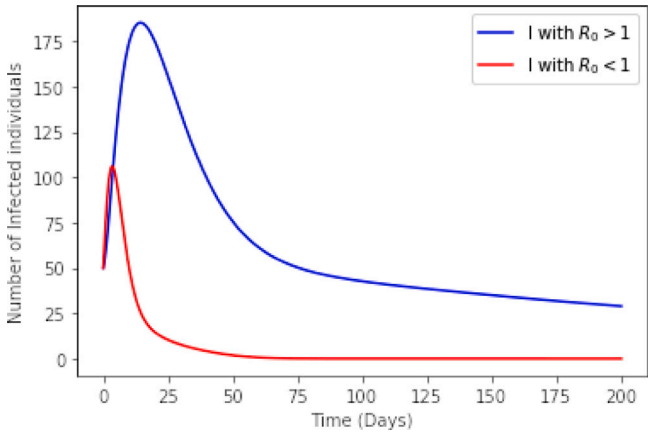

Fig. 11. Dynamics of infected individuals I with $\beta = \beta_0(1-\zeta\xi)(1-\kappa)(1-\upsilon)$.

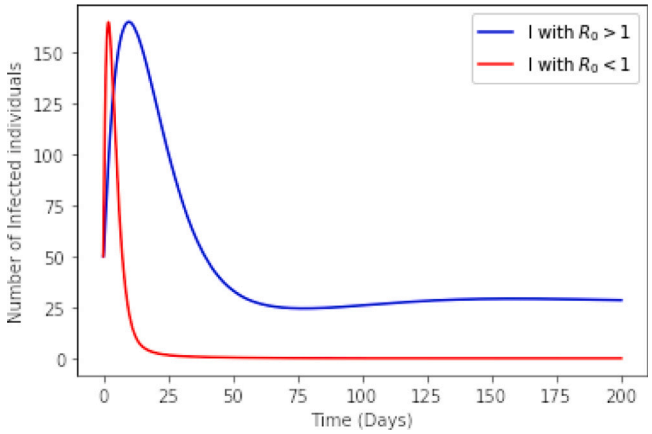

Fig. 12. Dynamics of infected individuals I with $\beta_I(t) = (\beta_f - \beta_0)e^{-r_1 t})$.

proportion implementing hand washing. It has been shown that R_0 is particularly sensitive to social/physical distancing and hand washing in this case [32]. On the other hand, assume $\beta = (\beta_0 - \beta_f)e^{-r_1 t} + \beta_f$ [33], where $\beta_0 = 0.2$ is the initial contact rate, $\beta_f = 0.77(> \beta_0)$ is the final contact rate, and $r_1 = 0.8$ is the exponential decreasing contact rate. The dynamics of the infective class in both cases depicted in Figs. 11 and 12 are somewhat similar, but the values of R_0 are different.

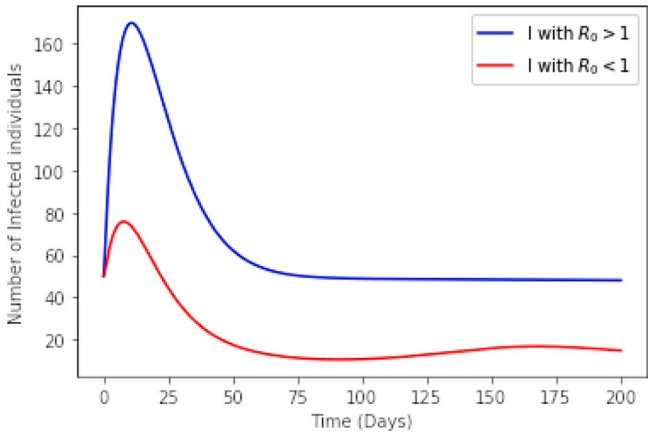

Fig. 13. Dynamics of infected individuals I with $\lambda_V = \sigma\beta_I I(1+\alpha_1 I)$ and $\lambda_S = \beta_I I(1+\alpha_1 I) + \beta_P P(1-p_P)(1+\alpha_2 P)$.

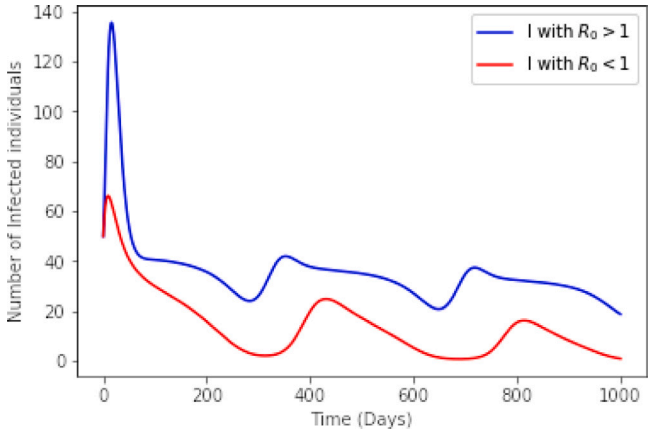

Fig. 14. Dynamics of infected individuals I with $\beta_I(t) = \beta_0 + \beta_0 sin\left(\frac{2\pi t}{365}\right)$.

Case 4: *Convex contact rate and seasonal variation* - We consider the following convex contact rate $\lambda_S = \beta_I I(1+\alpha_1 I) + \beta_P P(1-p_P)(1+\alpha_2 P)$, and $\lambda_V = \sigma\beta_I I(1+\alpha_1 I)$ [34], where $p_P = 0.77$ represents the proportion of individuals protected from environmental transmission [3], that is those practicing hand washing and disinfection of surfaces. Fig. 13 depicts this case. While the shape of the epidemic is similar to cases 1 and 2 above, we observe a little hump around day 125 of the epidemic when $R_0 < 1$, indicating that even though the epidemic has almost reach its disease-free equilibrium, a second wave could emerge. This is in line with the current dynamics of the Covid-19 pandemic as several countries are experiencing a second or third wave, while there was a believe that the disease was under control (due to strict lockdown measure after the first wave).

Effective disease contact rates are often driven by environmental factors such as seasonal variations. The seasonality is widely used in epidemic models, and it can make the system more complex, where nonlinear dynamics are found in the system. Even though the Covid-19 pandemic has been around for less than two years and seasonal variations are yet to be observed [35], we investigated the potential effect of seasonality on infection dynamics from the mathematical standpoint. Consider a contact rate including a *sine* function, commonly used to model periodic phenomena such as influenza-like epidemics $\beta(t) = \beta + \beta sin(\frac{2\pi t}{365})$ [15,36]. Fig. 14 shows as expected that the resonance effect tapers off with time, that is, the disease will taper off after about 3 years, indicating that the world might still be a long way off to see the end of this pandemic.

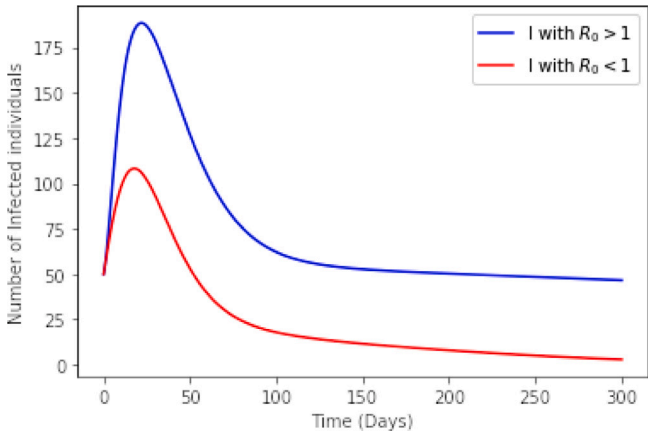

Fig. 15. Dynamics of infected individuals I with $\tau = \frac{1-CFR}{\tau_r}$ and $\mu = \frac{CFR}{\tau_d}$.

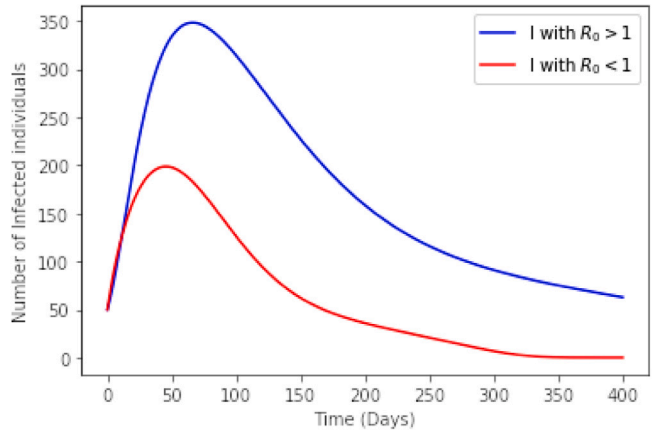

Fig. 16. Dynamics of infected individuals I with $\tau(t) = \tau_0(1 - e^{\tau_1 t}$ and $\mu(t) = \mu_0 e^{\mu_1 t}$.

Case 5: *Recovery and natural death rates depend on the infections fatality rate vs recovery and natural death rate are time dependent functions* - When the recovery and natural death rates depend on the infections fatality rate (CFR), these are respectively given by $\tau = \frac{1-CFR}{\tau_r}$, and $\mu = \frac{CFR}{\tau_d}$, where $CFR = 0.5\%, \tau_r = 10, \tau_d = 18$ (unit of τ_r, τ_d are days [37]. Fig. 15 depict this case. On the other hand, Fig. 16 is the graphical representation of the case when recovery and natural death rates are time dependent functions given by $\tau = \tau_0(1 - e^{-\tau_1 t})$, and $\mu = \mu_0 e^{\mu_1 t}$, with $\tau_0 = 0.6767, \tau_1 = 0.003, \mu_0 = 0.018, \mu_1 = 0.021$ [38]. One notes that the infections dies off quicker when case fatality rate is accounted for in Fig. 15 compared to when recovery and natural death rates are time dependent as shown in Fig. 16.

Finally, Covid-19 has affected healthcare resources (e.g., number of hospital beds) [39]. Thus, recovery rate could be considered as a linear incidence function which depends on the number of hospital beds, that is, $\tau(I, B) = \tau_0 + (\tau_1 - \tau_0)\frac{B}{I+B}$, where B is the hospital-bed to population ratio [40], τ_1 represents the maximum removal rate when the number of hospital beds sufficient, τ_0 represents the minimum per capita removal rate that can be sustained in the face of a large number of infections [40–42]. Graphical representation of this case is similar to Figs. 15 and 16 and for this reason is not represented here.

4. Conclusion

The novel and highly contagious coronavirus disease has rapidly spread across the globe, causing unprecedented socio-economic burden on communities. Several modeling studies have accounted for direct transmission in their mechanistic models. Herein, we formulated a deterministic Covid-19 model with both direct and indirect transmissions, and computed the basic reproduction number. The impact of indirect (human-to-environment) transmission is investigated, and results indicate that accounting for environmental perturbations has a clear impact on the disease dynamics as there are more infections than when indirect transmission is ignored. Consequently, additional strategies to mitigate the spread of the virus on surfaces such as disinfection will be required.

Next, because non-pharmaceutical control interventions are incorporated in several studies as a factor of the force of infection, we numerically investigate the effect of some of these functional forms on the contact and treatment rates on the disease spread when the basic reproduction number is either less or greater than unity. While the shape of most these graphs are similar (using the same model parameter values), key differences are the peak of the infection and the time to reach this peak, as well as the time when the hump tapers off.

One question was posed in this study. To determine whether the choice of the functional forms of the contact and treatment rates influence the long term dynamics of the disease. To better answer this question, we considered several forms of the contact rate. Numerical simulations were then carried out to investigate their impact on the disease dynamics. Results based on functional forms of the contact rates show some differences and could even substitute each other. Thus, the choice of the functional form of the effective contact rate has an impact on the dynamics of the infection. This highlights the importance of carefully accounting for the control measures being implemented prior to investigating their impact on the disease dynamics, as the choice and form of the contact rate should be specific to the prevention measures being implemented.

This study to qualitatively assessing via numerical simulations the impact of direct and indirect transmissions as well as the role played by the various forms of the contact and treatment/recovery rates is not exhaustive. A literature review of additional functional forms used in the literature could be conducted and compared as done herein. Early estimation and calibration of the model with observed (daily) epidemiological data is critical to provide data-driven information to public health and policy decision-makers at the onset of the epidemic/pandemic.

Declaration of competing interest

The authors declare that they have no known competing financial interests or personal relationships that could have appeared to influence the work reported in this paper.

Acknowledgments

Thanks the reviewers for their constructive comments.

References

[1] Al-Raeei Marwan. The COVID-19 basic reproductive ratio using SEIR model for the middle east countries and some other countries for two stages of the disease. Bull Natl Res Centre 2021;45(1):1–7.
[2] Lemos-Paiao Ana P, Silva Cristiana J, Torres Delfim FM. A new compartmental epidemiological model for COVID-19 with a case study of Portugal. Ecol Complex 2020;44:100885.
[3] David Jummy Funke, et al. Modeling the potential impact of indirect transmission on COVID-19 epidemic. MedRxiv 2021.
[4] Ahmed Jishan, et al. Effect of environmental and socio-economic factors on the spreading of COVID-19 at 70 cities/provinces. Heliyon 2021;7(5):e06979.
[5] Rong Xinmiao, et al. Effect of delay in diagnosis on transmission of COVID-19. Math Biosci Eng 2020;17(3):2725–40.
[6] Khan Muhammad Altaf, Atangana Abdon, Alzahrani Ebraheem. The dynamics of COVID-19 with quarantined and isolation. Adv Difference Equ 2020;2020(1):1–22.
[7] Oud Mohammed A Aba, et al. A fractional order mathematical model for COVID-19 dynamics with quarantine, isolation, and environmental viral load. Adv Difference Equ 2021;2021(1):1–19.

[8] Asamoah Joshua Kiddy K, et al. Global stability and cost-effectiveness analysis of COVID-19 considering the impact of the environment: using data from ghana. Chaos Solitons Fractals 2020;140:110103.
[9] Van Doremalen Neeltje, et al. Aerosol and surface stability of SARS-CoV-2 as compared with SARS-CoV-1. N Engl J Med 2020;382(16):1564–7.
[10] Memarbashi Reza, Mahmoudi Seyed Mahdi. A dynamic model for the COVID-19 with direct and indirect transmission pathways. Math Methods Appl Sci 2021;44(7):5873–87.
[11] Kassa Semu M, Njagarah John BH, Terefe Yibeltal A. Analysis of the mitigation strategies for COVID-19: from mathematical modelling perspective. Chaos Solitons Fractals 2020;138:109968.
[12] Mwalili Samuel, et al. SEIR model for COVID-19 dynamics incorporating the environment and social distancing. BMC Res Notes 2020;13(1):1–5.
[13] Akindeinde SO, Okyere E, Adewumi AO, Lebelo RS, Fabelurin OO, Moore SE. Caputo fractional-order $SEIRP$ model for COVID-19 pandemic. Alex Eng J 2021.
[14] Huang Jianzhe, Qi Guoyuan. Effects of control measures on the dynamics of COVID-19 and double-peak behavior in Spain. Nonlinear Dynam 2020;101(3):1889–99.
[15] Al-Arydah Mo'tassem, et al. Modeling cholera disease with education and chlorination. J Biol Systems 2013;21(04):1340007.
[16] Van den Driessche Pauline, Watmough James. Reproduction numbers and subthreshold endemic equilibria for compartmental models of disease transmission. Math Biosci 2002;180(1–2):29–48.
[17] Khajanchi Subhas, Bera Sovan, Roy Tapan Kumar. Mathematical analysis of the global dynamics of a HTLV-I infection model, considering the role of cytotoxic T-lymphocytes. Math Comput Simulation 2021;180:354–78.
[18] Kribs-Zaleta Christopher. Vector consumption and contact process saturation in sylvatic transmission of T. cruzi. Math Popul Stud 2006;13(3):135–52.
[19] Crawford Britnee, Kribs-Zaleta Christopher. A metapopulation model for sylvatic T. cruzi transmission with vector migration. Math Biosci Eng 2014;11(3):471.
[20] Aronna Maria Soledad, Guglielmi Roberto, Moschen Lucas Machado. A model for COVID-19 with isolation, quarantine and testing as control measures. Epidemics 2021;34:100437.
[21] Gonzalez-Parra Gilberto, Martinez-Rodriguez David, Villanueva-Mico Rafael J. Impact of a new SARS-CoV-2 variant on the population: A mathematical modeling approach. Math Comput Appl 2021;26(2):25.
[22] Agusto Folashade B, Gumel Abba B. Theoretical assessment of avian influenza vaccine. Discrete Contin Dyn Syst Ser B 2010;13(1):1.
[23] Elbasha Elamin H, Gumel Abba B. Theoretical assessment of public health impact of imperfect prophylactic HIV-1 vaccines with therapeutic benefits. Bull Math Biol 2006;68(3):577.
[24] Rabiu Musa, Willie Robert, Parumasur Nabendra. Mathematical analysis of a disease-resistant model with imperfect vaccine, quarantine and treatment. Ric. Mat. 2020;69(2):603–27.
[25] Ngonghala Calistus N, et al. Mathematical assessment of the impact of non-pharmaceutical interventions on curtailing the 2019 novel coronavirus. Math Biosci 2020;325:108364.
[26] Garba Salisu M, Lubuma Jean M-S, Tsanou Berge. Modeling the transmission dynamics of the COVID-19 pandemic in South Africa. Math Biosci 2020;328:108441.
[27] Alshammari Fehaid Salem. A mathematical model to investigate the transmission of COVID-19 in the Kingdom of Saudi Arabia. Comput Math Methods Med 2020;2020.
[28] Yang Chayu, Wang Jin. Transmission rates and environmental reservoirs for COVID-19 a modeling study. J Biol Dyn 2021;15(1):86–108.
[29] Riyapan Pakwan, Shuaib Sherif Eneye, Intarasit Arthit. A mathematical model of COVID-19 pandemic: A case study of Bangkok, Thailand. Comput Math Methods Med 2021;2021.
[30] Iboi Enahoro A, et al. Mathematical modeling and analysis of COVID-19 pandemic in Nigeria. MedRxiv 2020.
[31] Yafia Radouane. Modeling and dynamics in epidemiology, COVID19 with lockdown and isolation effect: Application to moroccan case. In: COVID19 with lockdown and isolation effect: Application to Moroccan Case (April 29, 2020). 2020.
[32] Ejigu Bedilu Alamirie, et al. Assessing the impact of non-pharmaceutical interventions on the dynamics of COVID-19: A mathematical modelling study in the case of Ethiopia. MedRxiv 2020.
[33] Beigi Alireza, et al. Application of reinforcement learning for effective vaccination strategies of coronavirus disease 2019 (COVID-19). Eur Phys J Plus 2021;136(5):1–22.
[34] ud Din Rahim, Algehyne Ebrahem A. Mathematical analysis of COVID-19 by using SIR model with convex incidence rate. Results Phys 2021;23:103970.
[35] He Shaobo, Peng Yuexi, Sun Kehui. SEIR modeling of the COVID-19 and its dynamics. Nonlinear Dynam 2020;101(3):1667–80.
[36] Trottier H, Philippe P. Deterministic modeling of infectious diseases: measles cycles and the role of births and vaccination. Internet J Infect Dis 2003;1(2).
[37] Paulo Claudio Moises, Fontinele Felipe Nunes, Cintra Pedro Henrique Pinheiro. Forecasting COVID-19 pandemic in mozambique and estimating possible scenarios. 2020, arXiv preprint arXiv:2007.13933.
[38] Fahmy Ahmed E, Eldesouky Mohammed M, Mohamed Ahmed SA. Epidemic analysis of COVID-19 in Egypt, Qatar and Saudi Arabia using the generalized SEIR model. MedRxiv 2020.
[39] Oliveira Juliane F, et al. Mathematical modeling of COVID-19 in 14.8 million individuals in Bahia, Brazil. Nature Commun 2021;12(1):1–13.
[40] Ajbar Abdelhamid, Alqahtani Rubayyi T, Boumaza Mourad. Dynamics of an SIR-based COVID-19 model with linear incidence rate, nonlinear removal rate, and public awareness. Front Phys 2021.
[41] Shan Chunhua, Zhu Huaiping. Bifurcations and complex dynamics of an SIR model with the impact of the number of hospital beds. J Differential Equations 2014;257(5):1662–88.
[42] Cui Qianqian, et al. Complex dynamics of an SIR epidemic model with nonlinear saturate incidence and recovery rate. Entropy 2017;19(7):305.